Ninth International Conference on
THIN-WALLED STRUCTURES – ICTWS2023
Sydney, Australia, Nov 29 – Dec 1, 2023

MOMENT CAPACITY OF NOVEL COLD-FORMED STEEL BUILT-UP BOX SECTIONS

Yecheng Dai*, Krishanu Roy, Gary M. Raftery*, and James B.P. Lim****

* Department of Civil and Environmental Engineering, The University of Auckland, New Zealand
e-mails: ydai151@aucklanduni.ac.nz, g.raftery@auckland.ac.nz

** School of Engineering, The University of Waikato, New Zealand
e-mail: kris.roy@waikato.ac.nz, james.lim@waikato.ac.nz

Keywords: Moment capacity; Cold-formed steel; Built-up box sections; Experimental tests; Finite element analysis.

Abstract. *This paper presents an experimental and numerical investigation conducted on novel unsymmetrical CFS built-up stiffened box section beams under bending. An elasto-plastic finite element (FE) model was developed and validated against the test results. The true material properties and initial geometric imperfections were considered in the FE models. The experimental results were also compared against the design moment capacities determined by the American Iron and Steel Institute (AISI S100) and Australian and New Zealand Standards (AS/NZS 4600). It was found that the moment capacities calculated from the AISI S100 and AS/NZS 4600 were conservative compared with the experimental results.*

1 INTRODUCTION

Cold-formed steel (CFS) members are popular in engineering practise due to their high recycling rate, ratio of strength to weight, stability, durability, and installation simplicity [1]. By joining multiple sections to create built-up sections, CFS members can now be used in large-span constructions, increasing their load-bearing capacity and stability. This approach has gained increasing interest in the industry at the moment. The CFS built-up sections connected with the help of several single sections at intermediate points, can take the form of various cross-sections, including back-to-back (BTB) built-up sections [2, 3] (see Fig. 1(a)), face-to-face (FTF) built-up box sections [4, 5] (see Fig. 1(b)), gapped built-up sections [6] (see Fig. 1(c)), angle built-up sections [7] (see Fig. 1(d)) and other cross-sectional shapes [8]. The structural behaviour of different CFS built-up box (CFSBB) sections has been examined in significant research papers that have been completed and are available in the literature.

Xu et al. [9] studied the moment capacity of face-to-face CFSBB sections, assembled by channels with and without lips, by conducting laboratory tests and numerical simulations. Screw connections were used to connect invidual channels. The impact of yield stress, the ratio of web height to section thickness, and connector position were studied by validated numerical models. Finally, the bending behaviour of such CFSBB sections, which was determined by adding the nominal strengths of each section, was advised to be modified by a factor of 0.9.

Laim et al. [10] carried out experimental tests under four-point bending and numerical simulations to explore the bending behaviour of CFSBB sections. A total of four channels were assembled to achieve such CFSBB sections (see Fig. 1(e)). A numerical simulation was conducted in comparison with the experimental results, and a parametric analysis was conducted to evaluate the effect of web height, section thickness, and member length on the flexural strength of CFSBB sections.

Wang and Young [11, 12] carried out tests and finite element modelling to explore the flexural strength of CFSBB sections having inward and outward web stiffeners (see Figs. 1(f) and (g)). The developed finite element (FE) models were validated with the test results. The impact of cross-sectional dimensions and location of screws was investigated. Modified equations based on the direct strength method were proposed for the moment capacity of CFSBB sections having inward and outward web stiffeners, respectively.

The flexural strength of CFSBB sections having a specific cross-sectional shape (see Fig. 1(h)) was experimentally and numerically investigated by Selvaraj and Madhavan [13]. Spot welding was used to connect individual single members at the junction of flange and lip. It was discovered that the design results were unsatisfactory and unconservative because the elastic buckling analysis had overestimated the buckling stresses and made an inaccurate prediction for the failure shape.

The research on the moment capacity of CFS-BTB built-up section beams was reported by Laim et al. [10], Wang and Young [11, 12] and Zhou et al. [14]. More recently, Ye et al. [15] performed a laboratory investigation to investigate the bending moment capacity of CFS-BTB unlipped channel sections subjected to combined distortional and local buckling. The design moment capacities predicted by Eurocode were found to provide accurate predictions, while the direct strength method provided rather conservative predictions.

With regards to CFSBB sections subjected to compression, innovative works were presented by Young and Chen [4]. The axial compressive behaviour of face-to-face CFSBB unlipped channel sections was experimentally studied. Intermediate stiffeners were designed on the web. The flexural strengths obtained from tests were in comparison with the flexural strengths obtained from DSM. The DSM buckling stress of such CFSBB sections achieved by using the sum of two single sections, was demonstrated to be conservative in general.

Li et al. [15] performed experimental tests and simulations to study the structural behaviour of face-to-face CFSBB lipped channel sections having multiple stiffeners on the web under axial compression (see Fig. 1(i)). The impacts of error for installation as well as connector distance on the axial compressive behaviour of such CFSBB sections were explored. New design equations for predicting the axial strength of such CFSBB sections was then provided.

Zhang and Young [16, 17] conducted experimental tests and FEA to explore the axial strength of face-to-face CFSBB unlipped channel sections with both inward and outward web stiffeners. A fix-ended boundary condition was used during the test, and member length was changed from 300 to 3200mm. The specimen failures comprised local buckling and combined local-flexural buckling. It was observed from the outcomes that the DSM was applicable when calculating the axial capacity of such CFSBB sections.

More recently, the study on the axial capacity of face-to-face CFSBB built-up box sections focused on different cross-sectional types, reported by Vy et al. [18, 19], Li and Young [20], and Selvaraj and Madhavan [21]. In addition, Dai et al. [22] used a deep learning approach and Genetic Algorithm to optimise four types of CFSBB sections subjected to axial compression. The data points used for the optimisation were achieved from the current design standards and FE models. A notable improvement of more than 180% in axial capacity was achieved compared to a practical CFSBB section.

Two types of novel unsymmetrical stiffened CFSBB sections, of which the overall web depth is up to 550 mm (see Fig. 2), have become popular for use as beam members recently [23] (see Fig. 3). However, the moment capacity of such CFSBB sections subjected to bending is not addressed in the current design standards comprising AISI S100 [24] and AS/NZS 4600 [25]. This is addressed herein. Firstly, new experimental test results on the moment capacity of such CFSBB sections under four-point bending were presented. FE models which considered

nonlinear material properties were then developed and verified with the experimental results, considering both the buckling shapes and moment capacity. The flexural strengths determined by the experimental tests and numerical analysis were also in comparison with the flexural strengths calculated using the DSM as recommended by AISI S100 [24] and AS/NZS 4600 [25].

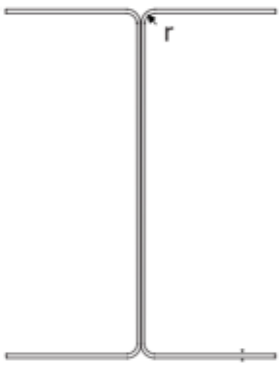	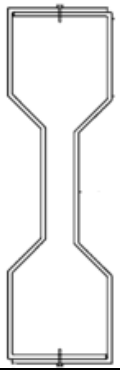	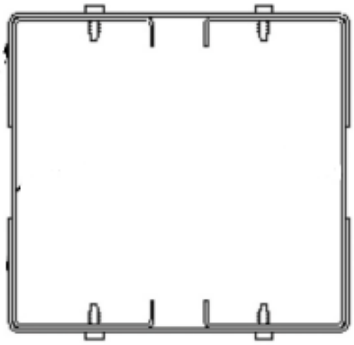
(a) Back-to-back built-up section [2]	(b) Face-to-face CFSBB section [4]	(c) Gapped CFSBB section [6]
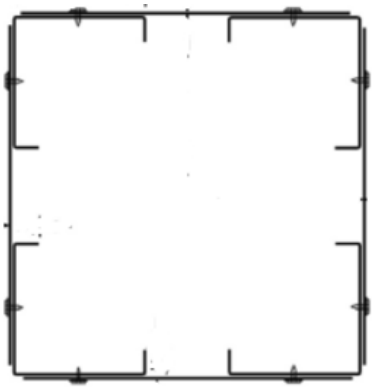		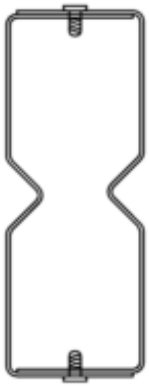
(d) Angle CFSBB section [7]	(e) Four-channel CFSBB section [10]	(f) CFSBB section with inward web stiffener [11, 12]
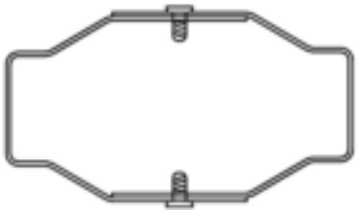	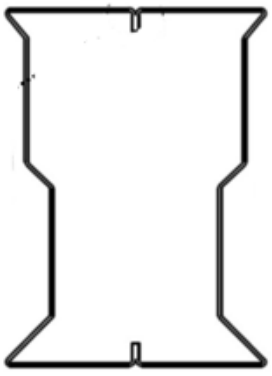	
(g) CFSBB section having outward web stiffener [11, 12]	(h) CFSBB section having specific shape [13]	(i) CFSBB section having multiple stiffeners on the web [15]

Figure 1: CFSBB sections reported by literature.

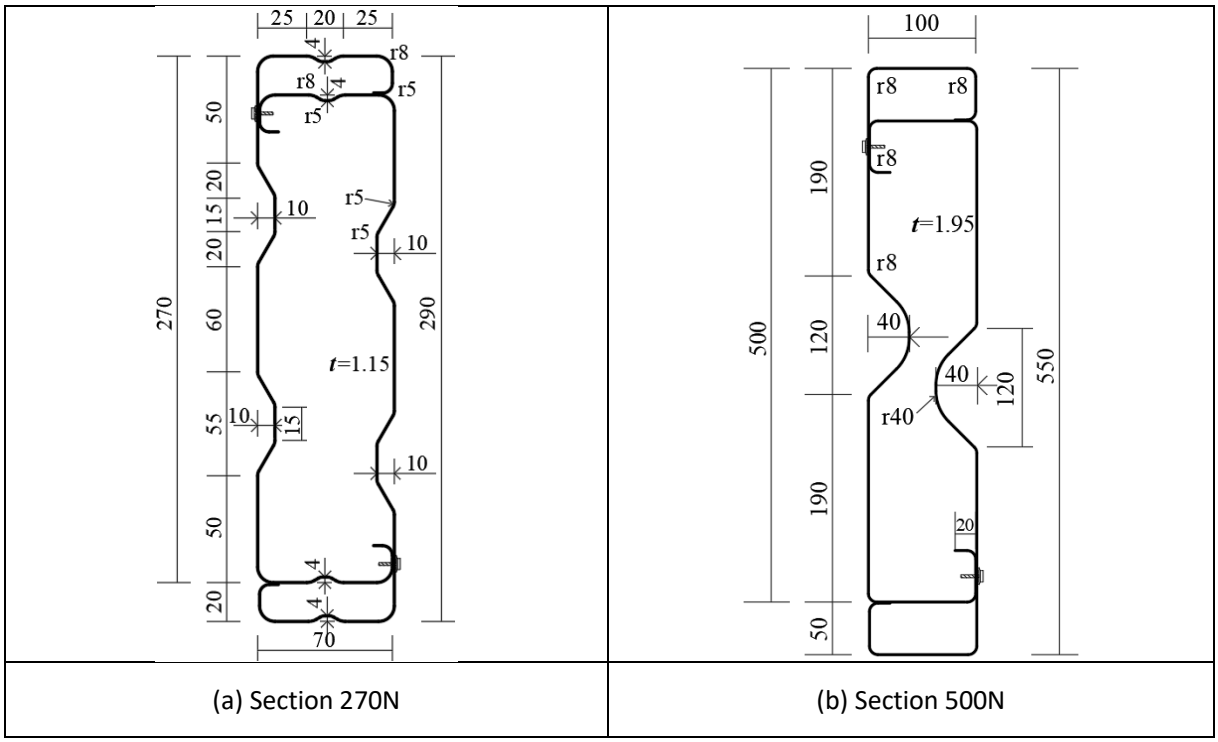

Figure 2: Dimensions of CFSBB sections in the current study. (units are mm) [5]

Figure 3: Practical CFSBB sections as beams. [5]

2 EXPERIMENTAL STUDY

In the current study, a total of 13 laboratory tests were conducted [26]. Various cross-sectional shapes, screw spacings and beam lengths were considered.

2.1 Testing process

The cross-sectional shapes included Section 270N (see Fig. 2(a)) and Section 500N (see Fig. 2(b)). Their overall web depths are 290 mm and 550 mm, respectively. Two same stiffened channels were assembled by self-tapping screws to fabricate a stiffened CFSBB section.

Prior to experimental testing, tensile coupon tests (see Fig. 4) were performed to acquire the true stress-strain relationships of CFSBB. In addition, the initial local and global geometric imperfections were acquired with the help of a laser scanner.

As displayed in Fig. 5, the specimens were tested under a four-point bending boundary condition. The lateral-torsional buckling was restrained using specifically designed lateral-restraints. Linear Variable Differential Transformers were utilised to record the vertical displacement. A similar experimental setup has been applied by past researchers [27].

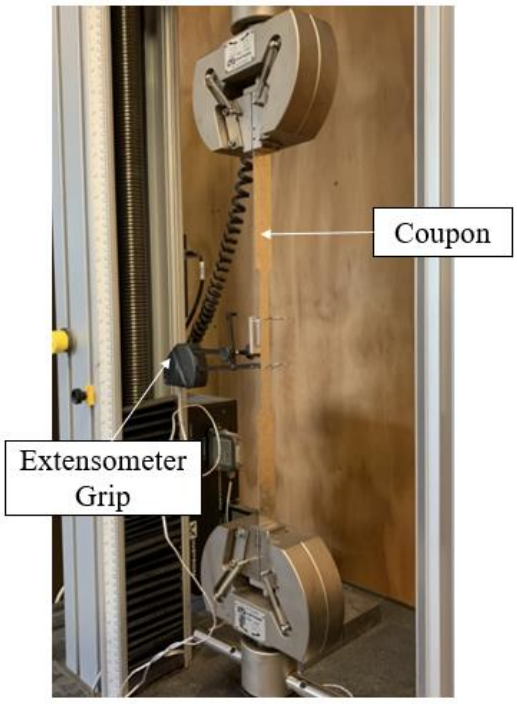

Figure 4: Setup of the tensile coupon test. [26]

Figure 5: Bending test setup. [26]

3 NUMERICAL STUDY

ABAQUS software [28] was utilised to model the bending test in this study. Similar modelling techniques has been reported in the literature [29].

3.1 Modelling details

The engineering stress-strain relationships achieved from the tensile coupon tests were converted to the true stress-strain relationships, which were then employed in ABAQUS [28]. The actual stress-strain relationships before the ultimate yield stress were used, and those after the maximum yield stress were not included in the plastic matrix of ABAQUS [28].

S4R elements were selected from the ABAQUS library [28] and then used for the CFSBB sections. C3D8R elements were employed to model the lateral-restraints. The same element type and meshing techniques have been used by past researchers [29].

Different lines were aligned on the surfaces of CFSBB sections. The positions of the intersections of various lines were consistent with the actual screw positions. It should be noted that the screws were not modelled using C3D8R solid elements, because no failure on the screws were observed. The type of "Catersian" beam connector was employed to model the self-tapping screws which were utilised in experimental tests.

The initial geometric imperfections were acquired using a laser scanner. The local and global imperfection magnitudes were employed as scale factors in the numerical simulations. The first-order buckling eigenmode was employed as the imperfection shape.

The relationship between contact surfaces was simulated using a "Hard contact". The boundary conditions applied on lateral-restraints were corresponding with the experimental boundary condition (see Fig. 6). More numerical simulation details could be found in [29].

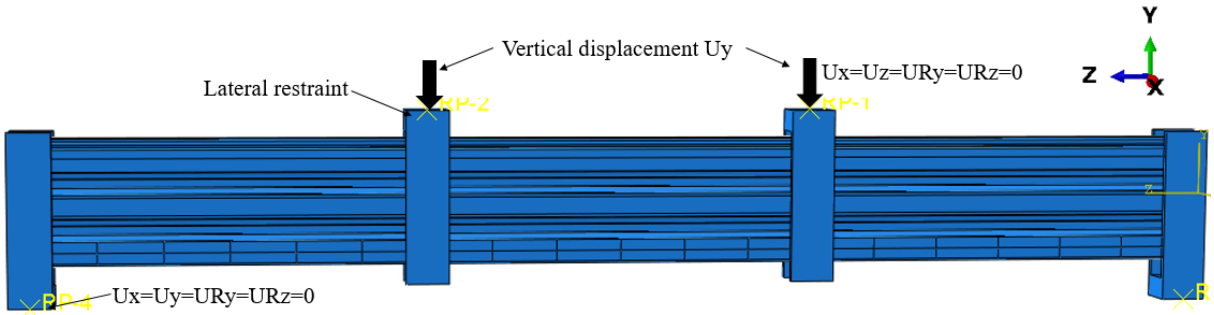

Figure 6: Boundary conditions in FEA. [26]

3.2 FE validation

The mean ratio of experimental flexural strengths to FEA strengths was found to be 0.97, and the coefficient of variation was 0.02 on average. It showed that the validated FE models were applicable in obtaining the moment capacity of stiffened CFSBB box sections investigated in the current study.

4 CURRENT DESIGN STANDARDS

4.1 Design equations

The direct strength method (DSM) as recommended by AISI S100 [24] and AS/NZS 4600 [25] was utilised to obtain the moment capacity of stiffened CFSBB sections.

For global buckling,

$$\text{When } F_o < 0.56F_y,\ F_{be} = F_o \tag{1}$$

$$\text{When } 0.56F_y \le F_o \le 2.78F_y,\ F_{be} = \frac{10}{9}F_y\left(1-\frac{10F_y}{36F_o}\right) \tag{2}$$

$$\text{When } 0.56F_y \le F_o \le 2.78F_y, \text{ For } 2.78F_y < F_o,\ F_{be} = F_y \tag{3}$$

For local buckling,

$$\text{For } \lambda_l \le 0.776,\ F_{bl} = F_{be} \tag{4}$$

$$\text{For } \lambda_l > 0.776,\ F_{bl} = \left[1-0.15\left(\frac{F_{ol}}{F_{be}}\right)^{0.4}\right]\left(\frac{F_{ol}}{F_{be}}\right)^{0.4} F_{be} \tag{5}$$

For distortional buckling,

$$\text{For } \lambda_d \le 0.673,\ F_{bd} = F_y \tag{6}$$

$$\text{For } \lambda_d > 0.673,\ F_{bd} = \left[1-0.22\left(\frac{F_{od}}{F_y}\right)^{0.5}\right]\left(\frac{F_{od}}{F_y}\right)^{0.5} F_y \tag{7}$$

4.2 Comparison of test results with design strengths

The mean ratio of experimental flexural strengths to the capacities determined by the DSM was 1.12. The DSM was found to offer conservative predictions for the stiffened CFSBB sections studied herein.

5 CONCLUSIONS

In this study, the flexural behaviour of novel unsymmetrical stiffened CFSBB sections was investigated through experimental tests and numerical simulation. The following conclusions can be drawn:

(1) The CFSBB sections were tested under four-point bending. Before bending tests, the true stress-strain relationships were achieved by conducting tensile coupon tests, and the initial geometric imperfections were recorded with the help of a laser scanner.

(2) FE models with nonlinear material properties were developed and verified against the experimental results. The verified FE models provided reliable predictions for the moment capacity.

(3) The experimental moment capacities were then in comparison with the design moment capacities determined by the DSM as presented in the AISI S100 and AS/NZS 4600. The design flexural strengths determined by the AISI S100 and AS/NZS 4600 were conservative compared with the experimental and FEA results.

NOMENCLATURE

CFS	Cold-formed steel;
CFSBB	CFS built-up box;
FE	Finite element;
F_{be}	Moment capacity when failure is by global buckling;
F_{bd}	Moment capacity when failure is by distortional buckling;
F_{bl}	Moment capacity when failure is by local buckling;
F_o	Buckling moment when failure is by global buckling;
F_{od}	Buckling moment when failure is by distortional buckling;
F_{ol}	Buckling moment when failure is by local buckling;

F_y	Yield strength;
λ_l, λ_d	Slenderness ratios;

REFERENCES

[1] Dai Y., Roy K., Fang Z., Raftery G.M., Ghosh K. and Lim J.B.P., "A critical review of cold-formed built-up members: Developments, challenges, and future directions", *Journal of Building Engineering*, **76**, 107255, 2023.

[2] Becque J. and Rasmussen K.J.R., "Experimental investigation of the interaction of local and overall buckling of stainless steel I-columns", *Journal of Structural Engineering*, **135(11)**, 1340-1348, 2009.

[3] Becque J. and Rasmussen K.J.R., "Numerical investigation of the interaction of local and overall buckling of stainless steel I-columns", *Journal of Structural Engineering*, **135(11)**, 1349-1356, 2009.

[4] Young B. and Chen J., "Design of cold-formed steel built-up closed sections with intermediate stiffeners", *Journal of Structural Engineering*, **134(5)**, 727-737, 2008.

[5] Dai Y., Roy K., Fang Z., Raftery G.M. and Lim J.B.P., "Web crippling resistance of cold-formed steel built-up box sections through experimental testing, numerical simulation and deep learning", *Thin-walled structures*, **192**, 111190, 2023.

[6] Meza F.J., Becque J. and Hajirasouliha I., "Experimental study of the cross-sectional capacity of cold-formed steel built-up columns", *Thin-walled structures*, **155**, 106958, 2020.

[7] Anbarasu M. and Dar M.A., "Improved design procedure for battened cold-formed steel built-up columns composed of lipped angles", *Journal of Constructional Steel Research*, **164**, 105781, 2020.

[8] Nie S., Zhou T., Eatherton M.R., Li J. and Zhang Y.., "Compressive behavior of built-up double-box columns consisting of four cold-formed steel channels", *Engineering Structures*, **222**, 111133, 2020.

[9] Xu L., Sultana P. and Zhou X., "Flexural strength of cold-formed steel built-up box sections", *Thin-walled structures*, **47**, 807-815, 2009.

[10] Laim L., Rodrigues P.C. and Silva L.S.D., "Experimental and numerical analysis on the structural behaviour of cold-formed steel beams", *Thin-walled structures*, **72**, 1-13, 2013.

[11] Wang L. and Young B., "Behavior of cold-formed steel built-up sections with intermediate stiffeners under bending. I: Tests and numerical validation", *Journal of Structural Engineering*, **142(3)**, 04015150, 2016.

[12] Wang L. and Young B., "Behavior of cold-formed steel built-up sections with intermediate stiffeners under bending. II: Parametric study and design", *Journal of Structural Engineering*, **142(3)**, 04015151, 2016.

[13] Selvaraj S. and Madhavan M., "Structural design of cold-formed steel face-to-face connected built-up beams using direct strength method", *Journal of Constructional Steel Research*, **160**, 613-628, 2019.

[14] Zhou X. and Shi Y., "Flexural strength evaluation for cold-formed steel lip-reinforced built-up I-beams", *Advances in Structural Engineering*, **14**, 4, 2011.

[15] Li Y., Li Y., Wang S. and Shen Z., "Ultimate load-carrying capacity of cold-formed thin-walled columns with built-up box and I section under axial compression", *Thin-walled structures*, **79**, 202-217, 2014.

[16] Zhang J.H. and Young B., "Experimental investigation of cold-formed steel built-up closed section columns withweb stiffeners", *Journal of Constructional Steel Research*, 14**7**, 380-392, 2018.

[17] Zhang J.H. and Young B., "Finite element analysis and design of cold-formed steel built-up closed section columns with web stiffener", *Thin-walled structures*, 131, 223-237, 2018.

[18] Vy S.T. and Mahendran M., "Behaviour and design of slender built-up nested cold-formed steel compression members", *Engineering structures*, 241, 112446, 2021.

[19] Vy S.T., Mahendran M. and Sivaprakasam T., "Built-up nested cold-formed steel compressionmembers subject to local or distortional buckling", *Journal of Constructional Steel Research*, 182, 106667, 2021.

[20] Li Q.Y. and Young B., "Experimental and numerical investigation on cold-formed steel built-up section pin-ended columns", *Thin-walled structures*, 170, 108444, 2022.

[21] Selvaraj S. and Madhavan M., "Design of cold-formed steel built-up closed section columns using direct strength method", *Thin-walled structures*, **171**, 108746, 2022.

[22] Dai Y., Roy K., Fang Z., Raftery G.M. and Lim J.B.P., "Optimal design of cold-formed steel face-to-face built-up columns through deep belief network and genetic algorithm", *Structures*, **56**, 104906, 2023.

[23] Formsteel Technologies Limited. (2018) Auckland, New Zealand.

[24] American Iron and Steel Institute, AISI. North American specification for the design of cold-formed steel structural members. Washington, DC: American Iron and Steel Institute; 2016.

[25] Australia/New Zealand Standard (AS/NZS), Cold-Formed Steel Structures, AS/NZS 4600:2018. Standards Australia/ Standards New Zealand, 2018.

[26] Dai Y., Roy K., Fang Z., Chen B., Hajirasouliha I., Raftery G.M. and Lim J.B.P., "Moment capacity of novel unsymmetrical cold-formed steel built-up stiffened box sections", to be submitted, 2023.

[27] Chen B., Roy K., Uzzaman A. and Lim J.B.P., "Moment capacity of cold-formed channel beams with edge-stiffened web holes, un-stiffened web holes and plain webs", *Thin-walled structures*, 1**57**, 107070, 2020.

[28] ABAQUS version 2022 [Computer software]. Dassault Systemes, Waltham, MA, 2022.

[29] Dai Y., Roy K., Fang Z., Chen B., Raftery G.M. and Lim J.B.P., "A novel machine learning model to predict the moment capacity of cold-formed steel channel beams with edge-stiffened and un-stiffened web holes", *Journal of Building Engineering*, 53, 104592, 2022.